Journal of Magnetics 6(1), 31-35 (2001)

Optimum Design of a Non-Destructive Testing System to Maximize Magnetic Flux Leakage

G. S. Park[1], P. W. Jang[2] and Y. W. Rho[3]

[1]*Dept. Electrical Engineering, Korea Maritime Univ., Pusan 606-791, Korea*
[2]*Dept. Physics, Chongju Univ., Chungbook 360-764, Korea*
[3]*KOGAS R&D Center, Ildong 638-1, Ansan city, Kyunggi-do, Korea*

(Received 14 September 2000)

This paper describes the design method of a magnetic system to maximize the magnetic flux leakage (MFL) in a non-destructive testing (NDT) system. The defect signals in a MFL type NDT system mainly depend on the change of the magnetic leakage flux in the region of a defect. The characteristics of the B-H curves are analyzed and a design method to define the operating point on B-H curves for maximum leakage is performed. The computed MFL signal by a nonlinear finite element method is verified by measurement using Hall sensors mounted on the 6 legs PIG, the traveling detector unit in gas pipe, in an 8 inch test tube with defects. The rhombic defects could be successfully identified from the defect signals.

1. Introduction

The magnetic flux leakage (MFL) type non-destructive testing (NDT) method is widely used to detect corrosion and other defects of the gas pipelines. The object pipeline is magnetically saturated by a magnetic system with permanent magnet and yokes. Hall sensors detect the leakage fields in the region of the defect. So, the sensitivity of the sensor system depends on the operating point in the magnetic saturation curves of the object, and on Hall sensor position.

To increase the sensing signals, it is necessary to increase the change of the magnetic leakage flux in the region of defect. In this paper, the optimal design method of the magnetic system with permanent magnet and yokes is described. In case the operating point on the magnetic saturation curves of the object is too low, the object will not be magnetically saturated in the defect region, so the defect signals become weak. In case it is too high, the change of the magnetic flux in the defect region will be small, so the amplitude of the sensor signal becomes weak again. The operating point of the magnetic system is optimized so as to maximize the change of the magnetic flux in the region of the defect. The computed MFL signal obtained by a nonlinear finite element method is verified by actual measurements. For the measurement, we made a gas pipe of 8 inches diameter with several types of artificial defects and on MFL PIG with 6 legs. In each leg, a magnetizing yoke and magnet was equipped with 3 sets of Hall sensors to detect the MFL signals. Artificial rhombic defects could be successfully identified from the defect signals.

2. Optimal Operating Points in Saturation Curves

Fig. 1 shows the conventional model of a cross section of a gas pipeline with a defect. In the figure, Φ_a is the magnetic leakage flux under the region without defect, Φ_c is the magnetic leakage flux under the region with defect and Φ_b, Φ_d are the fluxes inside the tube. The amplitude of the Hall sensor signal depends on the leakage flux density Φ_c. Not only the magnitude of Φ_c but the ratio Φ_c/Φ_a influences the signal to noise ratio of the defect detection system. Fig. 2

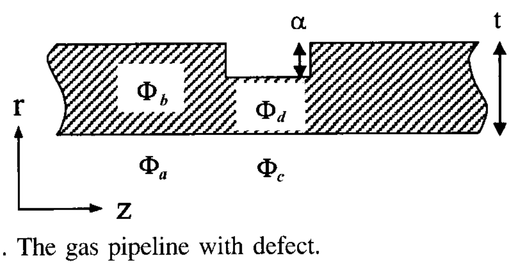

Fig. 1. The gas pipeline with defect.

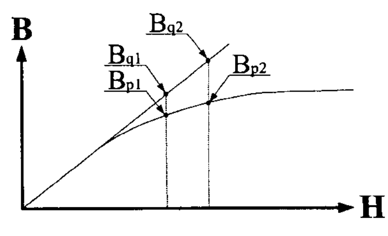

Fig. 2. The magnetic saturation curves.

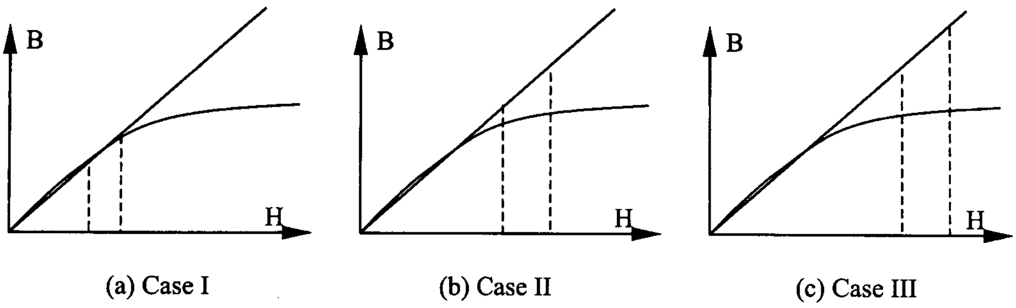

Fig. 3. Three cases of the operating point and λ.

shows the magnetic saturation curves of the object. In the region of a defect, the magnetic field is increased a little because of the defect depth. If the tube is not saturated, Φ_d is equal to Φ_b. So the magnetic flux density inside the tube is increased from B_{q1} to B_{q2}. If the tube is magnetically saturated, the remnant flux Φ_b-Φ_d will increase Φ_c. The magnetic flux density in this case is increased from B_{p1} to B_{p2}. The ratio Φ_c/Φ_a is defined with respect to the operating point in the saturation curves because of the non-linearity of the magnetic system. In Fig. 2, B_q-B_p is proportional to the leakage flux. So, we can define a leakage parameter λ that is proportional to Φ_c/Φ_a.

$$\lambda=\frac{B_{q2}-B_{p2}}{B_{q1}-B_{p1}} \tag{1}$$

Fig. 3 shows three possible cases. In case the operating point is too low, as in Fig. 3(a), the magnitude of Φ_c is small and so is λ. In case the operating point is too high as in Fig. 3(c), the magnitude of Φ_c is big, but the change of leakage flux Φ_c/Φ_a is small and so is λ. The optimum case is in Fig. 3(b). In this case, the operating point of the object is approaching saturation and a small defect will saturate the object so that the λ value is big. So, the design of the magnetic system with permanent magnet and yoke should be optimized to set the operating point in the region with high λ.

3. Finite Element Analysis

In an MFL type NDT, a Hall sensor detects the leakage field around a defect in the tested object. The field source is mainly a magnet assembled in the PIG. So it is a highly nonlinear system with permanent magnet. In this case, we cannot use the relation $B=\mu H$ anymore. The Maxwell equations in this nonlinear permanent magnet system would be as follows.

$$\nabla \times H=J \tag{2}$$

$$B = \mu_0(H+M) \tag{3}$$

$$B=\nabla \times A \tag{4}$$

So, the system equation is as follows,

$$H = vB-v_rM \tag{5}$$

$$\nabla \times (v\nabla \times A)=J+v_r\nabla \times M \tag{6}$$

$$-(\nabla \cdot v\nabla)A=J+v_r\nabla \times M \tag{7}$$

where v, v_r, J and A are the magnetic susceptibility, the relative susceptibility, the current density and the magnetic potential, respectively. In this equation, the susceptibility is not constant so that (7) needs to be solved iteratively. In case the tested object with defect is under-saturated, the magnitude of the magnetic leakage field will be small. In case the object is over-saturated, the change of the magnetic field around the defect will be small. So the sensitivity of the NDT depends on the operating point in the saturation curve of the tested object.

Fig. 4 shows typical flux distribution of the MFL type NDT in PIG. If we want to detect the depth a sensitively, the magnet size should be designed so that the operating point of the B-H curve is $p \cdot B_s$ where B_s is the saturation point of the magnet and p is the saturation factor. In the figure, the length of the magnet l_m is as in (8),

$$l_m=\frac{B_t}{p \cdot B_s} \cdot \frac{t}{1-\alpha/t} \tag{8}$$

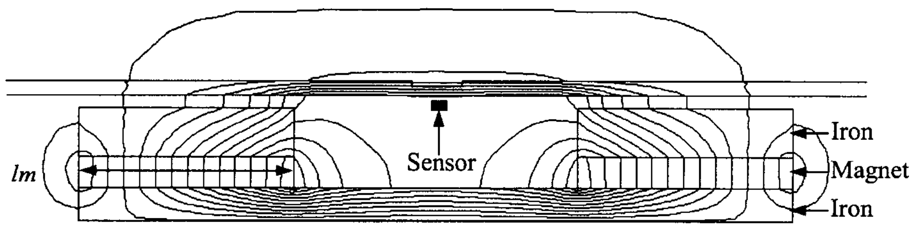

Fig. 4. Magnetic flux leakage computed by finite element analysis.

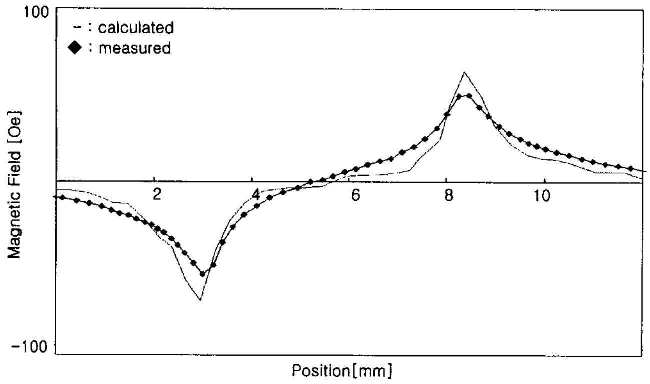

Fig. 5. Measured and calculated MFL signals. The depth of the defect is 1.74 mm and the length is 5.8 mm. (Thickness of the pipe t=5.8 mm)

where t is the thickness of the pipe, α the depth of defect or corrosion. The magnetic flux in the tube B_t and p is the target value in the design. The non-linear characteristics of the NdFeB magnet and steel pipe are analyzed iteratively.

4. Sensing Signals

For the measurement, we made a gas pipe of 8 inches diameter with several types of artificial defects and on MFL PIG with 6 legs. In each leg, the magnetizing yoke and magnet were equipped with 3 sets of Hall sensors. Fig. 5 shows the radial component of magnetic field. The thickness t of the pipe is 5.8 mm, the depth of the defect is 1.74 mm and the length is 5.8 mm. The magnitude and distance between peaks of the calculated signals are bigger than measured, as expected. As the depth of the defect increases, the magnitude of the sensing signal is also increasing as in Fig. 6. In this figure, the axial component B_z and the radial component B_r of the magnetic flux density are displayed for defect depths 0.58 mm, 1.74 mm and 5.22 mm, respectively. The computed magnitude of the MFL signals with respect to defect depths is compared with measurements in Fig. 7.

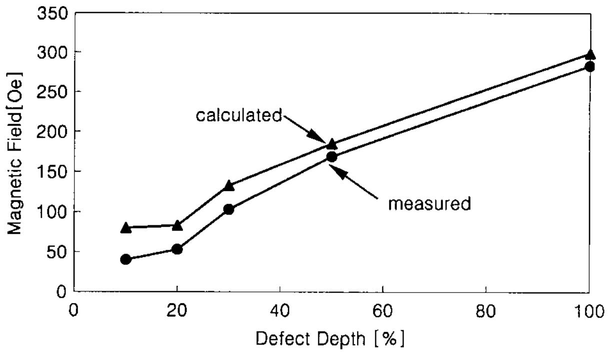

Fig. 7. The magnitude of the MFL signals with respect to defect depths.

5. Reconstructed Images of Defects

If we measure the defect signals with several positions of the sensor, the defect image can be constructed. Fig. 8(a) shows the sensing signals with axial and radial components from an artificial hollowed rhombic defect. Based on the signals of Fig. 8(a), the image of the hollowed rhombic defect can be constructed as in Fig. 8(b). Image constructions from the signals were performed with Matlab software. In case of grooved rhombic defects, the signals and the constructed images are in Fig. 9. In the figures, the radial component of the magnetic field gives better image than axial component.

6. Conclusions

Since the MFL type NDT system is a highly nonlinear magnetic system, the detected signal depends on the operating point of the magnet. In this paper, an optimum design method of the magnetic system to maximize the MFL signals in NDT is described. Since the sensitivity of the MFL sensor mainly depends on the change of the leakage flux, the design method is optimized to define the operating point in B-H curves for the maximum leakage. The computed MFL signal by a nonlinear finite element method is verified

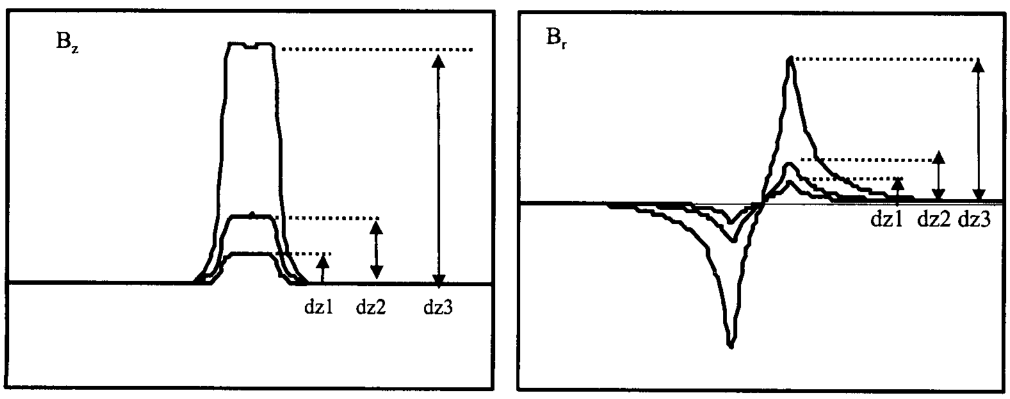

Fig. 6. Sensing signals with respect to the defect depths. (dz1 : 0.58 mm, dz2 : 1.74 mm, dz3 : 5.22 mm) The width of the defect remains constant. Bz is axial field and Br is radial field.

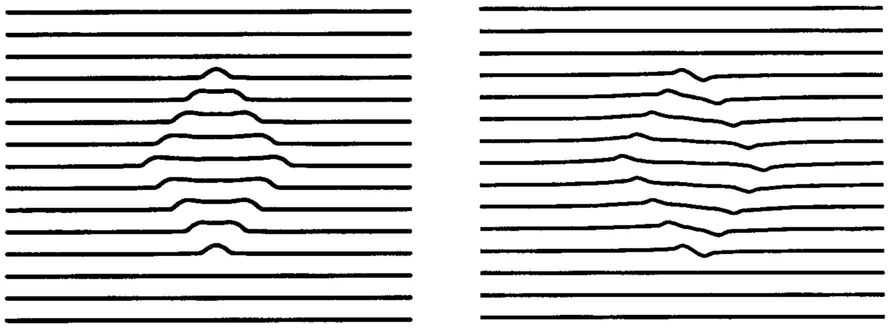

(a) Leakage flux of the axial and radial components from hollowed rhombic defect

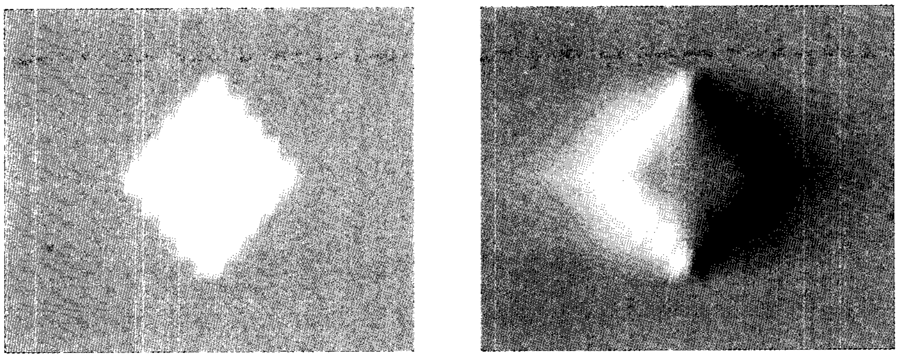

(b) Constructed images of the signals from hollowed rhombic defect

Fig. 8. Detected MFL signals and constructed images of an artificial hollowed rhombic defect. The size and depth of the defect is 3t x 3t and 0.9t. The size of the Hall sensor track space is 0.42t.

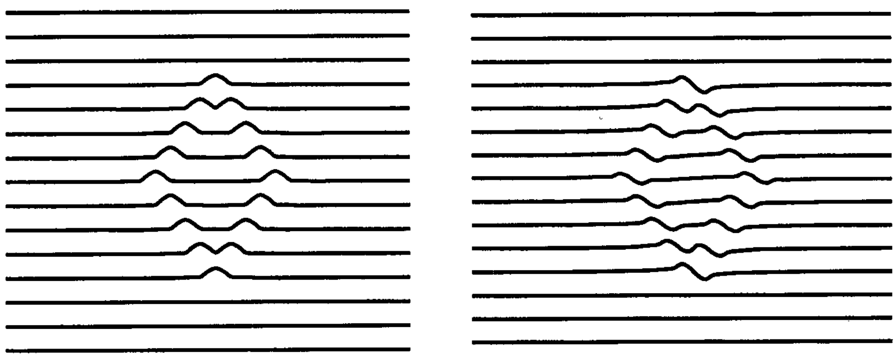

(a) Leakage flux of the axial and radial components from grooved rhombic defect

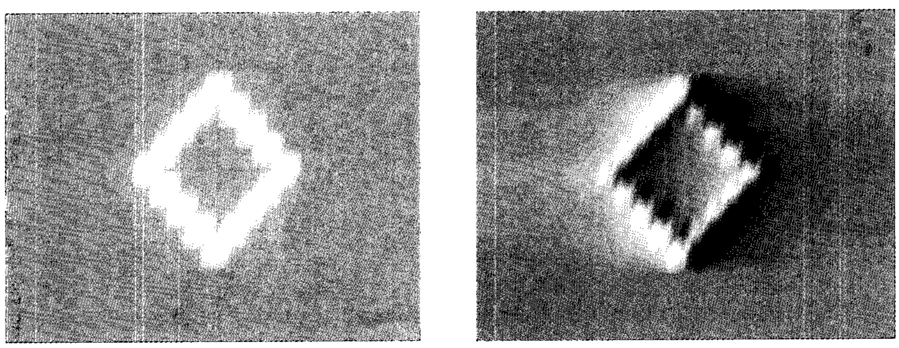

(b) Constructed images of the signals from grooved rhombic defect

Fig. 9. Detected MFL signals and constructed images of an artificial grooved rhombic defect. The size of the groove width is 0.5t.

by measurement using Hall sensors mounted on the 6 legs PIG in an 8 inch test pipe with defects. The rhombic defects could be successfully reconstructed from the defect signals.

References

[1] H. Haines *et al.*, "Advanced MFL signal analysis aids pipe corrosion detection", Pipeline & Gas Industry, 49 (1999).
[2] K. K. Tandon, "MFL Tool Hardware for Pipeline Inspec tion", Materials Selection & Design, 75 (1997).
[3] D. L. Atherton and M. G. Daly, "Finite Element Calcula tion of Magnetic Leakage Detector Signals", NDT Interna tional, **20**(4), 235 (1987).